Scouring Downstream of Sluice Gate

By

Siow-Yong Lim[1] and Guoliang Yu[2]

ABSTRACT

This paper presents the results of an extensive experimental study on local scour caused by high velocity jets issuing from submerged sluice gates or 2-D jet outlets. 84 sets of experiments have been conducted, out of which 63 sets were under deeply submerged jet conditions. Dimensional analysis is used to delineate the characteristic parameters affecting the maximum scour depth downstream of the structure. Under certain hydraulic conditions, the study discovered a cyclical jet-flipping phenomenon whereby the jet action would flip from the bed to the water surface and vice versa.

The erosion at the interface between the solid apron and the sand bed, i.e., at the brink of the apron was measured. The maximum brink scour depth, d_b, immediately at the downstream end of the apron was found to be about 0.44 times the maximum scour depth. For the prediction of the maximum scour depth, an empirical formula has been proposed, based on a database of 163 experiments from the present study and various other researchers. The formula takes into account the jet size and velocity, median sediment size, sediment density and gradation and the length of the protective apron. The formulation directly takes into account the effect of the apron length, which is a key parameter in the design of scour countermeasure for this type of problem. The range of applicability of the formula, and its uses and limitations has been discussed. The formula was used to estimate the scour caused by the high jet velocity issuing from the sluice gate of the Shimen Arch Dam in China and the prediction was close to the measured scour in the field.

INTRODUCTION

Water releases at high flow velocity through hydraulic structures, such as sluice gates or spillways, may cause stability problem of the riverbed downstream of the structure. To protect the structures, a typical engineering solution is to build a solid apron downstream of the structures in order to minimize the effect of erosion from the structures. However, local scour downstream of the apron may still occur even though most of the flow energy has been appropriately dissipated over the length of the apron. The scour depth not only depends on the impinging flow velocity, characteristics of bed material, but also the apron length and apron surface roughness. The optimum apron length is a key parameter in the design of this type of scour countermeasures. It is therefore necessary to study the effect of apron on the scour depth. Since the initial investigation of water jet scouring by Rouse (1939) and Laursen (1952), numerous experiments have been carried out to study

[1] Associate Professor, School of Civil & Environmental Engineering, Nanyang Technological University, Nanyang Avenue, Singapore 639798. csylim@ntu.edu.sg
[2] Research Fellow, School of Civil & Environmental Engineering, Nanyang Technological University, Nanyang Avenue, Singapore 639798.cglyu@ntu.edu.sg

the scouring phenomenon. For 2-D jets without an apron, these include the works by Tarapore (1956), Valentin (1967), Basmaci (1971), and Rajaratnam (1981), Ali and Lim (1986). Other investigators have studied the influence of a rigid protective apron on the bed scouring, such as Iwagaki et al (1965), Hassan and Narayanan (1985), Chatterjee et al (1994), Li (1993), Aderibigbe and Rajaratnam (1998).

A few empirical models have been proposed for the prediction of the maximum scour depth for jet scour phenomena. These models were mainly based on the densimetric particle Froude number, opening size of the jet, and uniform sediment size. Aderibigbe and Rajaratnam (1998) found that the non-uniformity of the sediment has a significant effect on the size of the scour hole produced by the jet.

The primary objective of this study is to investigate the bed scouring caused by flow issuing from a sluice gate or 2-D horizontal water jets from a nozzle. The flow may or may not initially flow over a protective apron before reaching the erodible bed. Extensive experimental investigations have been carried out to study the jet flow characteristics and the bed scouring using different apron lengths and bed material sizes under varying flow conditions. Dimensional analysis is used to delineate the characteristic parameters affecting the flow patterns and the maximum scour dimensions of the hole created by the jet flow.

EXPERIMENTS

The experiments were conducted in the Hydraulics Laboratory at NTU. Two flumes were used and the experimental set up is shown in Figs. 1a and 1b. The large glass-wall flume (Fig. 1a) measures 20m long, 0.494m wide and 0.688m deep and the water is released from a well-rounded vertical sluice gate installed near the upstream end of the flume. The small glass-wall flume (Fig. 1b) measures 8m long, 0.2m wide and 0.3m deep. In the small flume, in addition to using the sluice gate, a specially designed shoe-shaped nozzle made of stainless steel was also used to issue a 2-D horizontal wall jet. The rational behind using the nozzle was to overcome the physical constraint of the small flume. The flume is only 0.3 m deep; hence, it is difficult to produce a jet of high velocity from the small difference in head upstream and downstream of the sluice.

In both flumes, a solid Perspex platform approximately 4m long was constructed to simulate a rigid apron. The sluice gate or nozzle can be installed at any location on the apron. This arrangement facilitates the study of the effect of apron length on the scouring downstream of the gate.

A sediment recess area followed the end of the apron. This was filled with the bed material and flushed level with the apron. In the small flume, the sediment bed was 10cm deep and 2m in length, while in the large flume, the sediment bed was 25cm deep and 5m in length. The arrangements assured that each equilibrium scour hole formed would not hit the bottom of the flume. Seven different types of uniform quartz sediments were used as bed material. The median size of the sediments varies from 0.68 mm to 4.92 mm. The geometric standard deviation of the sediments varies from 1.17 to 1.33.

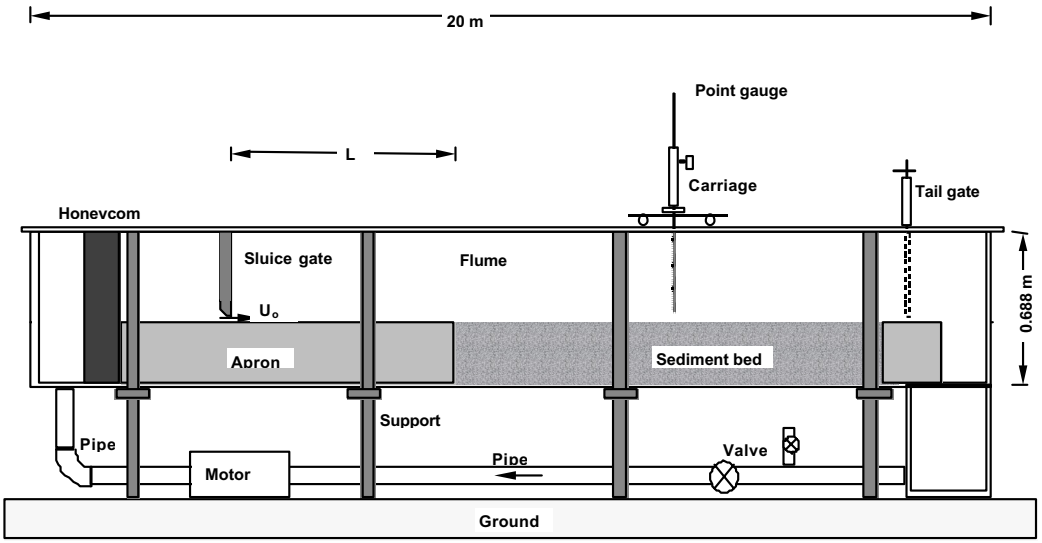

Figure 1a. Layout of experimental set-up in the big flume

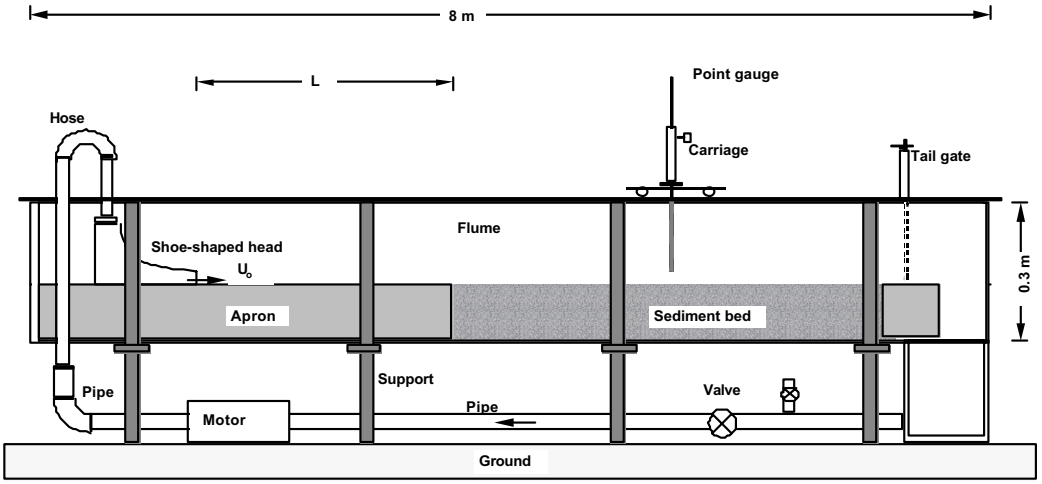

Figure 1b. Layout of experimental set-up in the small flume

Altogether, 84 sets of experiments were conducted, out of which 63 sets were under deeply submerged jet conditions, i.e., the tailwater depths were larger than 10 times the size of the jet opening. The experiments covered a wide range of jet velocities, apron lengths and sediment sizes and the range of the test conditions are listed in Table 1.

Table 1 Summary of the experimental conditions for the present study

No of Runs	d_o (mm)	d_{50} (mm)	σ_g	L (mm)	U_o (m/s)	S	F_o	d_{se} (mm)
14	3	0.68-4.92	1.17-1.24	0-180	0.92-1.37	2.65	3.26-10.58	14.5-61.0
48	10	0.82-2.94	1.14-1.33	0-900	0.34-2.45	2.65	2.95-11.23	6-185
7	20	2.66	1.34	0	0.71-1.77	2.66	3.41-8.50	62-210
15	26	1.82	1.22	0-1040	0.42-1.31	2.65	2.45-7.66	37-143.5

The procedure for each run is similar. Before each run was started, the sediment bed was leveled so that it was flushed with the rigid apron. The sluice gate or nozzle was installed by shifting to the desired distance from the sediment bed. The pump was turned on and the flow was adjusted to a pre-determined flow rate using a flow meter connected in the supply pipeline. The flow rates were checked regularly to ensure the consistency of the flow. At the end of the flume, a tailgate was adjusted so that the tailwater depth was maintained at a high level to achieve a 2-D fully submerged horizontal jet. The experiments were usually conducted for days or even several weeks until no significant changes in the scour profile were observed. During the run, the scour profiles along the centerline were measured at regular time interval using a point gauge attached to a traversing carriage that could slide along the two rails on the top of the flume. The time evolution of the scour profiles along the sidewall was also recorded on transparencies pasted on the glass wall.

SCOURING PROCESSES

Fig. 2 shows a definition sketch of the scour hole formation downstream of the apron. In general, the scouring process is such that once the jet discharging from the sluice gate or nozzle comes into contact with the erodible bed, a lot of sand particles are eroded and transported downstream. During the process a scour hole and a crest are formed. During the initial stage, the rate of scouring is very rapid. As time increases, the rate would decrease and eventually approaches zero as the equilibrium scour hole is reached. For a typical scouring process, the three observable stages of scouring are: (i) an initial stage with rapid rate of scouring; (ii) a development or erosion stage which has a relatively slower rate of scouring; (iii) an equilibrium stage where there are no observable changes in the scour depth after a long scouring time.

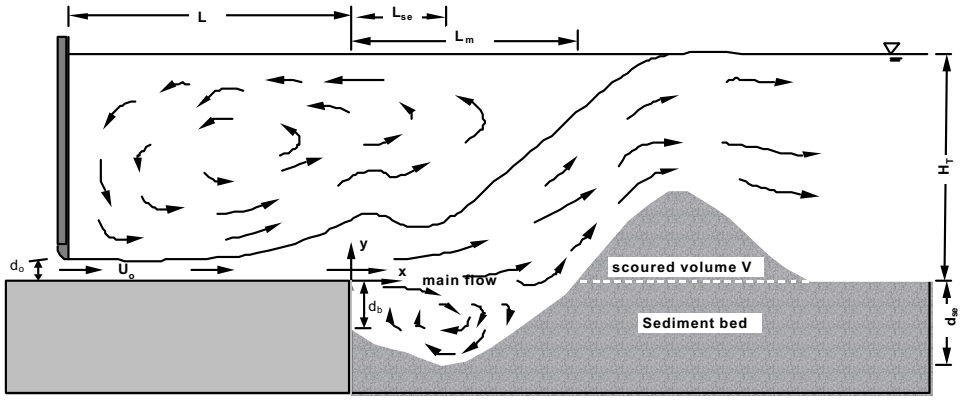

Fig. 2. Definition sketch of scour below a sluice with an apron

At the equilibrium stage, the scour hole would have attained its maximum depth. Though there were no observable changes in depth, the scour hole continued to lengthen and simultaneously shifting the crest further downstream. At the same time, the sand particles around the region of the maximum scour depth would roll to and forth without causing any deepening of the scour hole. At the end of the experiment, it was observed that, even for the uniform sediment used, the crest was covered by a layer of relatively finer particles and upstream of the crest, the particles were coarser. The coarsest particles were located around the region of the maximum scour depth. While proceeding further upstream towards the rigid apron, the particle sizes were finer again.

In some experiments, it was observed that the discharging jet from the sluice gate was unstable during the scouring process. The jet axis was observed to be 'oscillating' between a position along the bottom of the scouring bed and a position in the horizontal direction. Figs. 3 to 5 show these jet positions and the interaction of the jet with the erodible bed. The oscillation period was generally between 5 to 10 seconds.

When the jet was attached to the bed (Fig. 3), it eroded and transported a lot of particles, some of which (mainly finer particles) were transported over the dune or while others were swept upstream by the reverse flow. The coarser particles were mainly deposited and piled at the downstream end of the scour hole, resulting in the thickening of the coarser layer and the steepening of the bed slope, which was supported by the jet. Once the steepness of the bed exceeded a certain limit, the jet could no longer support the bed and it was forced to impinge on a section of the scour hole. While doing so, it strongly eroded the bed and generated a sediment cloud immediately downstream of it.

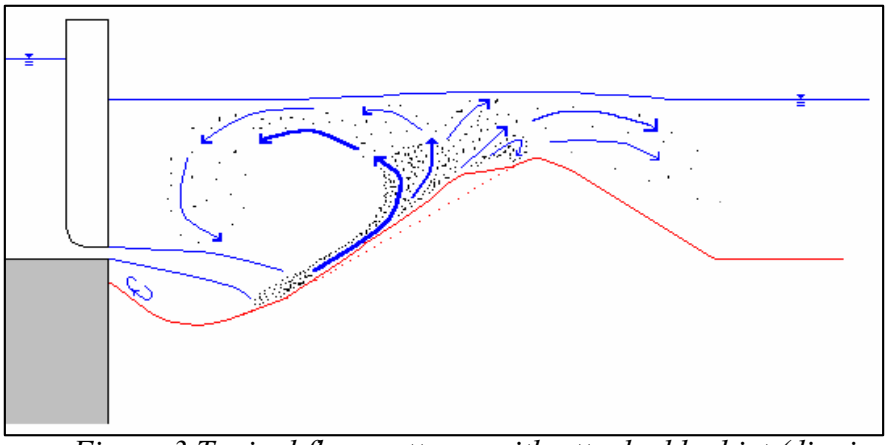

Figure 3 Typical flow patterns with attached bed jet (digging phase)

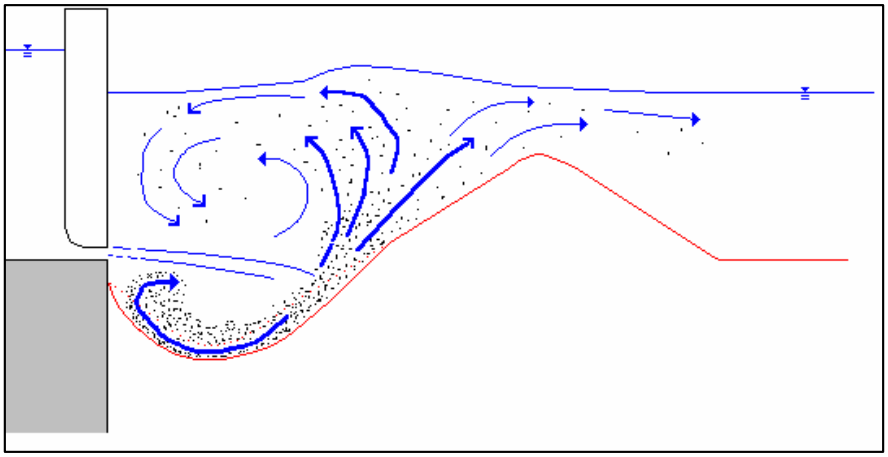

Figure 4. Typical flow patterns with the jet rising to the surface

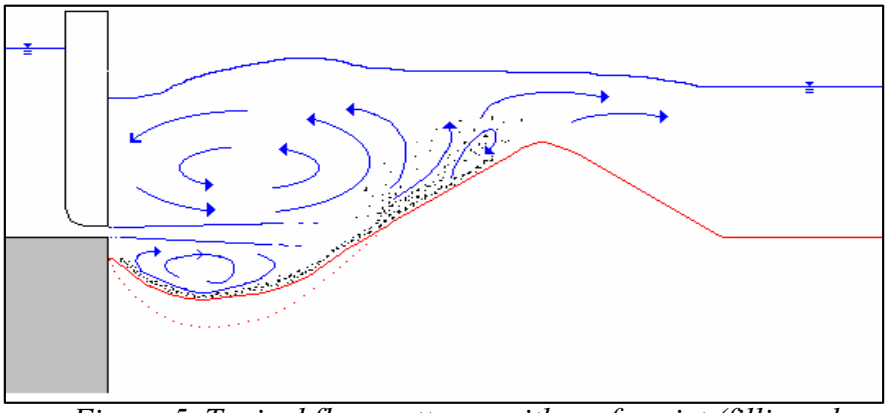

Figure 5. Typical flow patterns with surface jet (filling phase)

The maximum scour depth occurred during the jet impingement (Fig. 3) and it was referred to as the deeper dynamic scour depth (digging phase). A sediment-laden vortex was formed upstream between the bed and the jet. The jet then started to rise (Fig. 4) towards the horizontal position, causing the impingement area to move downstream into the sediment deposits which at the same time were being transported along the bed and

back into the mid section of the scour hole. By the time the impingement area had reached the end of the scour hole, that is, when the jet path was horizontal, all the sediment deposits were back in the mid-section of the scour hole (filling phase). The maximum scour depth at this point was referred to as the shallower dynamic scour depth (Fig. 5). This process was continuously repeated, resulting in a scour hole with mainly coarser particles and a dune covered by finer particles. Though the armor layer was never stable, the scouring process was assumed to reach equilibrium state when the scour hole did not show any significant change in depth during the digging phase.

The water surface profile also changed during the two phases. During the digging phase the water surface was very calm (Fig. 3), whereas during the filling phase the water surface was characterized by rippling profile as though the water was boiling (Fig. 4). As a result of the filling and digging actions at the scour hole zone, a shallower dynamic scour depth and a deeper dynamic scour depth were produced, respectively. When the jet was stopped the static profile of the eroded bed lay in between the two dynamic scour depths and this is recorded as the equilibrium scour depth.

CENTERLINE SCOUR PROFILES

Fig. 6 shows a typical time development of the centerline scour profiles caused by the submerged wall jet with an apron length 30 times the jet opening size. The scour profiles show that the scour patterns are rather similar in shape. In the past, Laursen (1952), Tarapore (1956), Rajaratnam (1981), Hassan and Narayanan, (1985) Ali and Lim (1986) and Chatterjee et al (1994) have shown that the scour patterns caused by jets were similar in shape as the scour progressed.

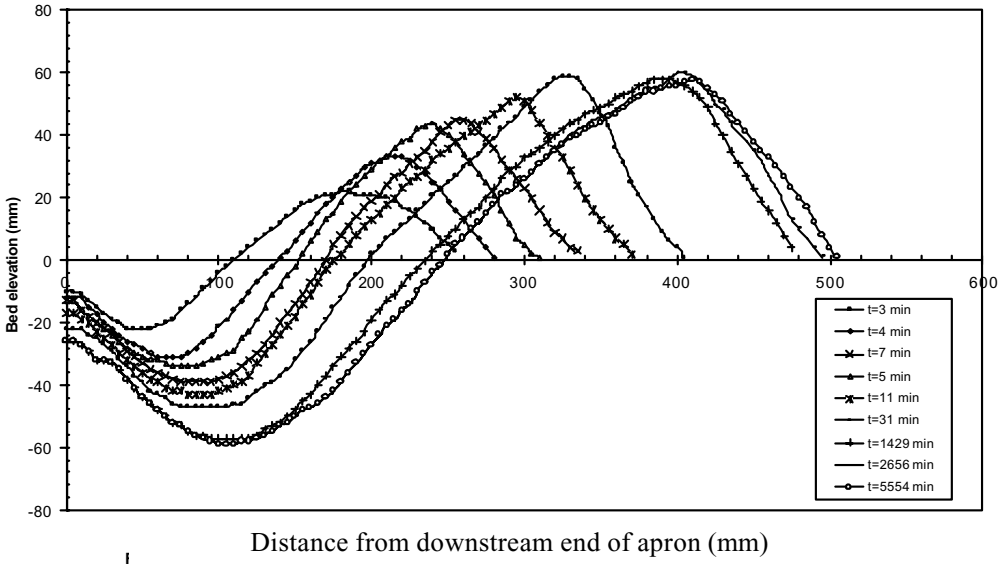

Figure 6 Centerline scour profiles, L = 300mm, d_o = 10 mm, U_o = 1.18 m/s, d_{50} = 2.94mm, H_t/d_o = 24.3 (Run SPB 4)

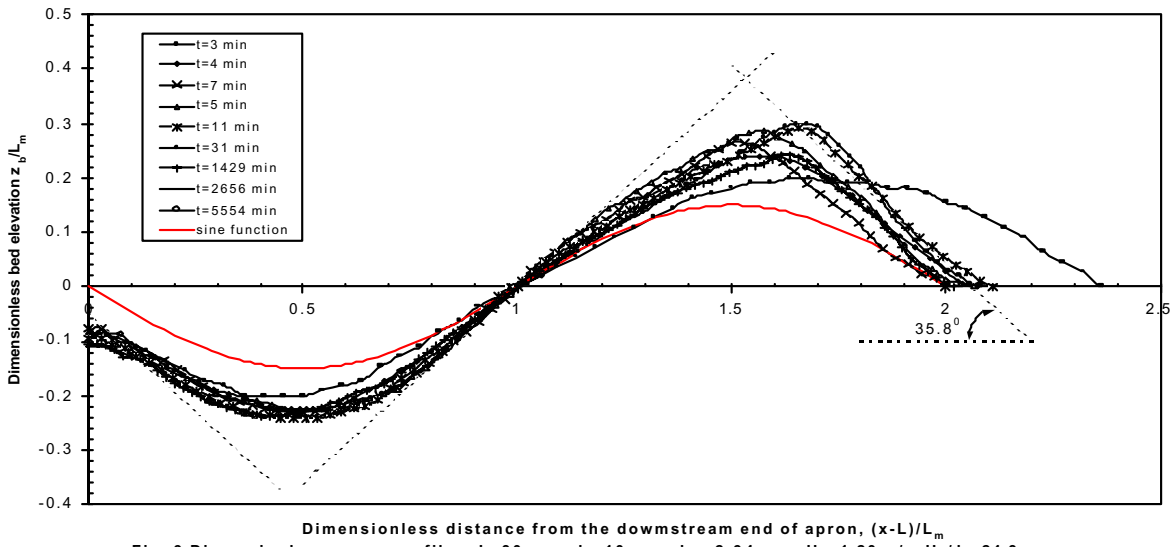

Figure 7 Similarity of centerline scour profiles, L = 30mm, d_o = 10 mm, U_o = 1.18 m/s, d_{50} = 2.94mm, H_t/d_o = 24.3 (Run SPB 4)

This means that using the proper scaling lengths; the scour profiles could be described by a single parameter. The scaling parameters used were different for different researchers. In this study, the scaling length used is L_m, which is the temporal length of the scour hole (see Fig. 2). Fig. 7 shows the dimensionless plot of z_b/L_m versus $(x-L)/L_m$ for the profiles in Fig. 6, where z_b is the scour depth at any x-distance in the scour hole. Except for the profiles in the first few minutes of scouring action, the figure shows that the plotted data could satisfactorily be represented by one curve, especially for the scour hole part of the eroded bed profiles. The profile resembles that of a sine function, which is superimposed on the figure.

The angle of repose for the sediment (=35.8^0) used was also calculated and superimposed on the figure. Generally, it can be seen that the upstream slope of the scour hole is slightly steeper than the downstream one. However, the downstream slope of the scour hole and the upstream slope of the ridge were quite close to the angle of repose.

MAXIMUM EQUILIBRIUM SCOUR DEPTH

There are a number of parameters that will affect jet scour in an alluvial bed, listed as follows,

$$d_{se} = f_1(\nu, \rho, \rho_s, d_{50}, \sigma_g, H_t, k_e, U_o, L, d_o, g) \qquad (1)$$

where d_{se} = maximum equilibrium scour depth, U_o = mean jet velocity at the efflux section, L = length of apron, d_o = jet opening size, H_t = tailwater depth, d_{50} = median sediment diameter, k_e = roughness height of the apron, ? = kinematic viscosity of fluid, ρ = fluid density, ρ_s = sediment density, σ_g = standard deviation of particle size distribution, g = gravitational acceleration. Using dimensional analysis, Eq. (1) becomes

$$\frac{d_{se}}{d_o} = f_2\left(\mathrm{Re} = \frac{U_o d_o}{\nu}, \frac{d_{50}}{d_o}, \frac{k_e}{d_o}, S = \frac{\rho_s}{\rho}, \sigma_g, \frac{H_t}{d_o}, \mathrm{Fr} = \frac{U_o}{\sqrt{g d_{50}}}, \frac{L}{d_o}\right) \quad (2)$$

Some of the terms in Eq. (2) may be dropped or combined with the following reasoning. First, the jet velocity is usually relatively high and the corresponding Reynolds number will therefore be much greater than a few thousands. This means the effect of the viscosity on the jet hydraulics and its scouring should be insignificant. Second, the apron roughness parameter, k_e/d_o may be neglected since the apron surface is relatively smooth and the apron length is also comparatively short in terms of energy dissipation on the apron surface compared to the energy lost due to the vortices generated. Third, the flow Froude number Fr and specific gravity of sediment S can be combined to form a sediment densimetric Froude number, F_o. Fourth, only data with deep tailwater submergence will be used in the analysis, i.e., with H_t/d_0 greater than 10. Hence, Eq. (2) becomes

$$\frac{d_{se}}{d_o} = f_3\left(\frac{d_{50}}{d_o}, \frac{H_t}{d_o}, F_o = \frac{U_o}{\sqrt{(S-1) g d_{50}}}, \frac{L}{d_o}, \sigma_g\right) \quad (3)$$

To evaluate the function, a database of 163 sets of flume data have been collected, out of which 63 data sets were from the present study and 100 sets were from other researchers. A summary of the experimental conditions is listed in Table 2. The data cover a wide range of flow and sediment conditions, and there are 61 sets of experiments with the installation of an apron downstream of the jet exit. Using regression technique, the dimensionless maximum scour depth is obtained as follows:

$$\frac{d_{se}}{d_o} = 1.04\, \sigma_g^{-0.69}\, F_o^{1.47} \left(\frac{d_o}{d_{50}}\right)^{-0.33} e^{-0.04\,\beta\left(\frac{L}{d_o}\right)^{1.4}} \quad (4)$$

where $\beta = \sigma_g^{-0.5} F_o^{-0.35} \left(\frac{d_o}{d_{50}}\right)^{0.5}$. Fig. 8 shows comparisons between the calculated and measured d_{se}/d_o. The comparison indicates that 76% of the data were within the ± 20% error band and 91% were within ± 30% error band. Eq. (4) includes the effects of the flow, jet size, sediment characteristics, and length of the protective apron. For example, for the same sediment size, the scour depth would decrease by about 50% if σ_g were increased from 1.2 to 3.13. This is consistent with the findings of Aderibigbe and Rajaratnam (1998).

Eq. (4) also indicates that the scour depth would decrease rapidly as the protective apron length increases. However, the deduction of the scour depth vis-à-vis the apron length is not a simple function of the latter. It is also associated with the jet size, flow and sediment characteristics as indicated by the factor β in Eq. (4).

Table 2 Summary of data from present study and other sources

Researchers	No of Run	d_o (mm)	d_{50} (mm)	σ_g	d_o/d_{50}	L/d_o (mm)	U_o (m/s)	S	F_o	d_{se}/d_o
Present Study	63	3-20	0.68-4.92	1.17-1.34	0.61-11.2	0-90	0.34-2.45	2.65	2.95-11.2	0.6-19.5
Rajaratnam (1981)	14	3.56-24.9	1.2-2.38	1.2*	1.5-10.5	0	0.87-2.22	2.65	4.43-14.0	3.34-31.29
Basmaci (1971)	13	3.74-12.62	1.3-6.50	1.2*	0.95-9.71	0	0.55-1.92	1.30-2.60	3.85-13.3	3.57-29.26
Iwagaki et al (1965)	19	5-20	1.85-3.75	1.2*	2.7-5.41	8-16	0.5-3.32	2.61	2.93-13.74	2.65-27.04
Tarapore (1956)	7	3.18	0.70-4.4	1.2*	0.72-4.54	0	0.85-1.86	2.65	6.97-12.16	11.72-28.48
Aderibigbe & Rajaratnam (1998)	32	5-25	1.15-6.75	1.32-3.13	0.74-31.7	0	0.58-4.77	2.65	2.78-29.46	1.32-32.74
Chatterjee et al**, (1994)	15	20-50	0.76-4.3	1.22-1.43	4.65-39.5	22-33	0.4-2.125	2.63-2.65	2.38-11.68	0.882-4.205

** σ_g is assumed to be 1.2 because the value was not given in the original source, but the bed material was mentioned as uniform;*

*** Efflux velocities were calculated from the discharges per meter width and the height of jet, given in Table 2 of Chatterjee et al (1994).*

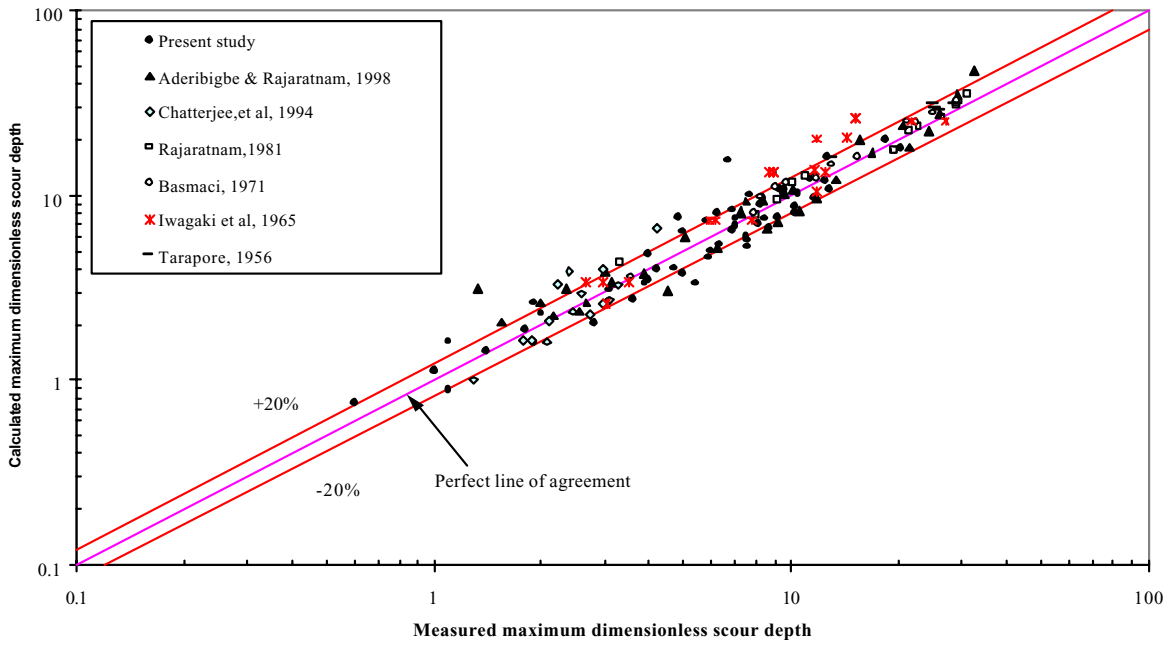

Figure 8 Comparison between calculated and measured dimensionless maximum scour depth, d_{se}/d_o for cases with and without aprons

When there is no apron installation after the jet opening, i.e., $L/d_o = 0$, Eq. (4) becomes

$$\frac{d_{se}}{d_o} = 1.04\ \sigma_g^{-0.69}\ F_o^{1.47} \left(\frac{d_o}{d_{50}}\right)^{-0.33} \tag{5}$$

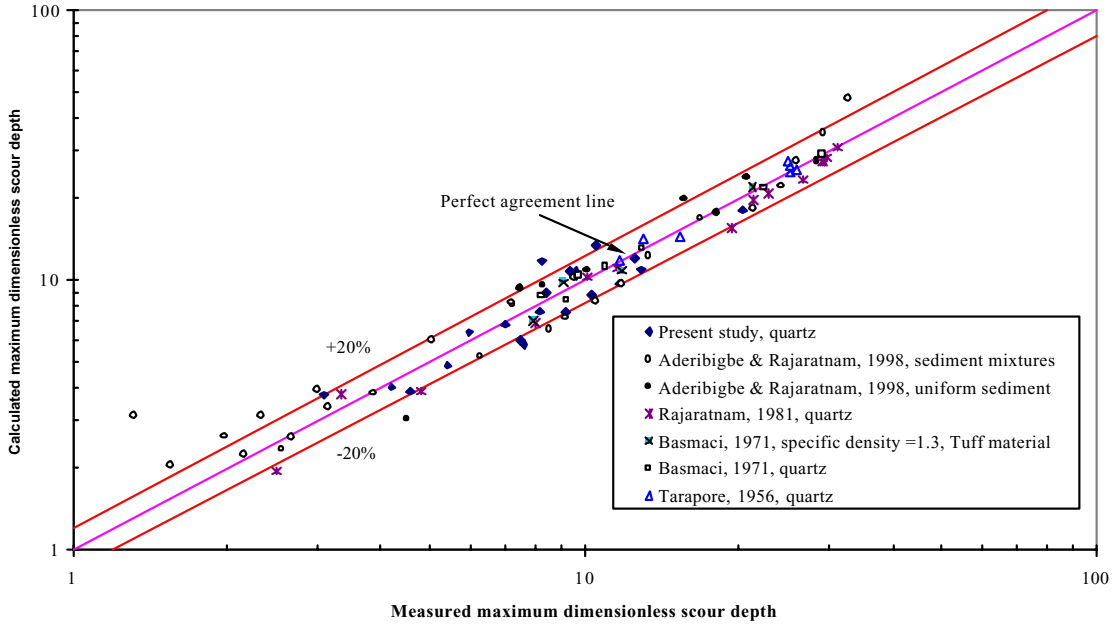

Figure 9 Comparison between calculated and measured dimensionless maximum scour depth, d_{se}/d_o for cases without apron

Fig. 9 shows the good agreement between the measured scour depth data without apron installation compared to the computed values using Eq. (5). 79.5% of the data tested were within the ± 20% error band and 94.4% of data tested were within the ± 30% error band. Note that the database used for Fig. 9 includes experiments conducted with tuff material where the specific gravity is equals to 1.3.

MAXIMUM BRINK SCOUR DEPTH

The erosion at the interface between the solid apron and the sand bed, i.e., at the brink of the apron is also of concern to the engineers. The reverse flow in the toe region immediately downstream or brink of the apron causes this to occur. The maximum brink or backwater scour depth, d_b, (see Fig. 2) at the downstream end of the apron base is also measured and evaluated in this study. As shown in Fig. 10, the maximum brink or backwater scour depth, d_b, is linearly related to the maximum scour depth, i.e.,

$$d_b = 0.44\, d_{se} \tag{6}$$

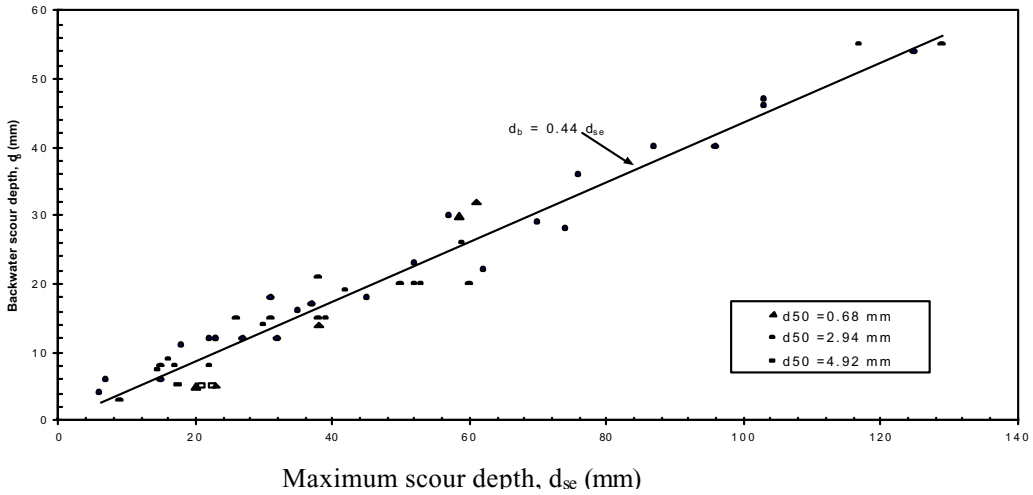

Figure 10 Relationship between maximum brink or backwater depth with maximum scour depth

FIELD APPLICATION

It is important to check if the proposed equation is applicable to field condition. An interesting field study on the Shimen Arch Dam by Li and Li (1999) provided the opportunity to test the formula. The Shimen Arch Dam was built in China along the Bao River in 1973. The structure has a 20m apron downstream of the six sluice gates (each with dimensions of 7m wide × 8m high) as shown in Fig. 11. In 1978 the apron protection was extended by 30 m to give a total apron length of 50m. The average slope of the apron floor is 7.6%, starting at elevation 535.8m and ending with an elevation of 530.0m. The head of water from the bottom of the sluice gates is about 22m.

In the period from 14 to 25 August 1981, the river was inundated with a one in 300 years flood flow and the water released from the 6 gates was as high as 4,840 m^3/s. Scouring occurred downstream of the sluice gates and the maximum scour depth recorded was about 13.6m, below the original bed level of the downstream channel. The mean efflux jet velocity at the entrance to the apron floor was estimated to be about 20.8-25.4 m/s, based on the head of water upstream of the sluice gates. This is consistent with the physical model measurements by Li and Li (1999). The mean flow field and the near bed velocities in bracket at three locations along the apron are also shown in Fig. 11. The mean efflux flow depth was estimated to be 4.03m, based on the flood discharge and the apron width. With a downstream water depth of about 53 m, the efflux flow can be considered as a deeply submerged jet.

The bed material downstream of the dam consists of layers of cipolin or quartzite. Each layer is less than 10 m thick. The high-speed flow destroyed the rocky layers into loose pieces of rock blocks. Some of these rocks were flushed out by the flow and formed the scour hole during the floods. According to the survey on the bed material in the scour hole, it was found that the rock blocks have a volume varying between 24 to 26 m^3. Taking the mean of 25 m^3 and assuming it to be spherical would give the bed material size a value of 3.62 m in diameter. We further assumed the bed material in the scour hole was quite uniform with σ_g = 1.2. With the above considerations and using Eq. (4), we obtained the computed maximum scour depths of between 12.9m to 17.0m for the velocity range of 20.8 to 25.4 m/s at the entrance section to the apron. Hence, the mean

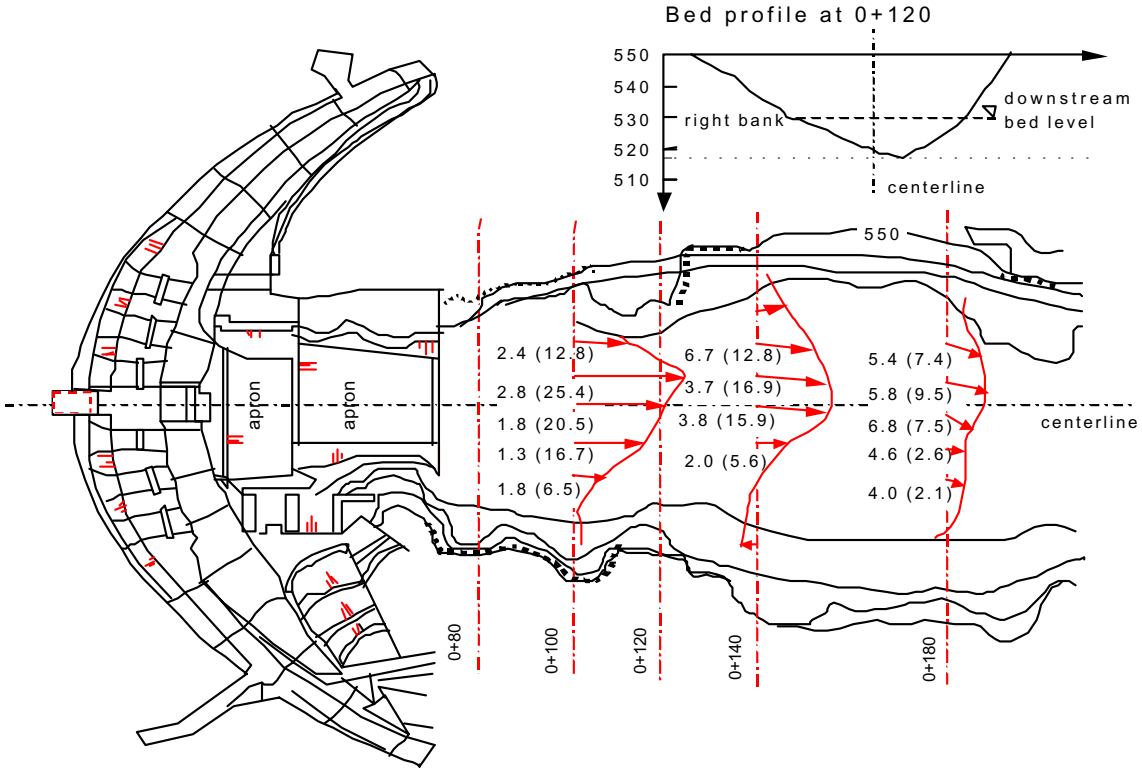

Figure 11 Structural layout of Shimen Arch Dam, the flow field and bed profile at maximum scour location (after Li and Li, 1999)

scour depth is 14.95m, and this value compares favorably with the measured maximum scour depth of 13.6m in the field.

RANGE OF APPLICABILITY

In this study, a formula (Eq. 4) has been proposed for the prediction of the maximum scour depth downstream of a submerged sluice gate or two-dimensional jet with an apron. The formula has considered most of the major factors affecting the formation of the scour

hole, such as the jet opening size, velocity, sediment size and gradation, and length of apron. The ranges of the pertinent parameters are: $2.38 \leq F_o \leq 29.46$, $0 \leq L/d_o \leq 90$, $0.61 \leq d_o/d_{50} \leq 39.5$, $1.3 \leq S \leq 2.65$, $1.17 \leq \sigma_g \leq 3.13$. Nevertheless, some aspects need to be discussed for future study and application.

First, the influence of the non-uniformity of bed material on the scour depth needs to be studied because the range of the geometric standard gradation of the bed material used in the database is not extensive. The second aspect to consider is the sediment size. The database is limited to jet scour with median sand size larger than 0.68 mm. The third is the influence of the tailwater depth. In the present analysis, this effect is neglected and the database considers only cases where the jet is fully submerged with tailwater depths greater or equal to 10 times the jet opening size. The proposed equation is therefore applicable to deeply submerged jets. In addition, Eq. (4) assumes the roughness on the rigid apron surface is smooth and would not affect the subsequent scour formation. However, if the apron surface is very rough, for example, with baffles on the apron floor for energy dissipation, Eq. (4) may give an over estimation of the scour depth.

Finally, the scattering of the experimental data in Fig. 8 may be due to systematic errors. As discussed earlier, the jet-flipping phenomenon causes the bed to be in a state of dynamic equilibrium between the filling and the digging phase. For these experiments, the largest scour depth is during the dynamic digging phase and this value is used in the analysis. This is consistent with the data provided by Aderibigbe and Rajaratnam (1998) where the dynamic maximum scour depths were measured at the end of the bed digging action. It should be mentioned that most of the other researchers adopted the time-averaged maximum scour depths. Using the data from the present work and Aderibigbe and Rajaratnam (1998), it is estimated that the two different measuring methods of the maximum scour depth may have contributed about ±15% of the systematic errors. From the viewpoint of engineering safety, we suggest that a safety factor of 1.3 should be considered when applying Eqs. (4) or (5) into field practices.

CONCLUSIONS

1. Generally, the bed scouring progress can be characterized into the three different stages, i.e., an initial stage where the scour rate is very rapid, a developing stage, and an equilibrium stage whence the maximum scour depth is attained. The time to achieve the equilibrium stage typically takes a few days to reach.
2. Under certain hydraulic conditions, a jet-flipping phenomenon was discovered in the present study. The process is cyclical. The jet would first act as an attached bed jet digging at the bed and creating a scour hole. When the hole had attained a certain depth, the bed jet would abruptly flip towards the water surface and transforms into a surface jet. At this instant, the digging action stopped abruptly and the sediment was observed to be back-filling from the ridge region into the scour hole. When the scour hole was almost leveled, the surface jet would transform into a bed jet again. The cyclical process of jet flipping from the bed (digging action with a calm water surface) and to the free surface (back-filling action with "boiling" water surface) was observed throughout the full duration of the experiment.

3. The time development of centerline scour profiles was found to be similar using the length of the scour hole as the scaling parameter.
4. The maximum brink scour depth at the toe of the apron was evaluated and found to be about 0.44 times the maximum scour depth.
5. Using a database consisting of 163 data sets from the present study and various researchers, an empirical formula (Eq. 4) has been proposed for the prediction of the maximum scour depth downstream of a submerged sluice gate or 2-D wall jets with or without a protective apron. The formula takes into account the jet size and velocity, median sediment size, sediment density and gradation and the length of the apron.
6. The formula was used to estimate the scour downstream of the sluice gate of the Shimen Arch Dam in China and the prediction was close to the measured scour in the field.

REFERENCES

1. Ade, F. and Rajaratnam, N. (1998). "Generalized study of erosion by circular horizontal turbulent jets." *J. Hydr. Res.*, IAHR, 36 (4), 613-635.
2. Aderibigbe, O. and Rajaratnam, N. (1998). "Effect of Sediment Gradation on Erosion by Plane Turbulent Wall Jets." *J. Hydr. Engrg.*, ASCE, 124 (10), 1034-1042.
3. Ali, K.H.M. and Lim, S.Y. (1986). "Local scour caused by submerged wall jets." *Proc. Instn. Civ. Engrs*, Part 2, 81, 607-645.
4. Basmaci, Y. (1971). "Localised scour under vertical gates by submerged jets." MSc Thesis, Middle East Tech. Univ., Turkey.
5. Chatterjee, S.S., S. N. Ghosh, and M. Chatterjee (1994). "Local scour due to submerged horizontal jet." *J. Hydr. Engrg.* ASCE, 120 (8), 973-992.
6. Hassan, N. M. K. and Narayanan, R (1985). "Local Scour Downstream of an Apron." *J. Hydr. Engrg*, ASCE, 111 (11), 1371-1385.
7. Iwagaki, Y., Tsuchiya, Y., and Imamura, M. (1965). "Studies of the Local Scour from Flows Downstream of an Outlet (1)." *Disaster Prevention Research Institute*, Annuals No. 8, Kyoto University, Japan, 363-377.
8. Laursen, E.M. (1952). "Observations on the Nature of Scour." *Proc. Fifth Hydr. Conf.*, Bulletin 34, University of Iowa, USA, 179-197.
9. Li, B.H. and Li, Z. (1999). "Three Dimensional Flow and Scour in the Energy Dissipation Zone of Shimen Arch Dam." *Journal of Water Power*, No. 12 (in Chinese).
10. Li, W. (1993). "Scour of Fine Sediment by a Turbulent Wall Jet*" Ph D Thesis*, Lamar University, Texas, USA.
11. Rajaratnam, N. (1981). "Erosion by plane turbulent wall jets" *J. Hydr. Research,* IAHR, Vol. 19, No. 4, 339-357.
12. Rouse, H. (1939), "Criteria for similarity in transportation of sediment." State University of Iowa Bulletin, 20, 33-39.
13. Tarapore, Z.S. (1956). "Scour below a submerged sluice gate." M Sc Thesis, University of Minnesota, USA.
14. Valentin, F. (1967). "Considerations Concerning Scour in the case of Flow under Gates." *Proc.12th Congress*, IAHR, Vol.3, 92-96.